

厚生労働科学研究費補助金（第3次対がん総合戦略研究事業）
分担研究報告書

チロシンホスファターゼの異常と発がん、浸潤・転移

研究分担者 的崎 尚 神戸大学大学院医学研究科 シグナル統合学分野 教授

研究要旨 チロシンリン酸化シグナルの制御には、チロシンキナーゼと共にチロシンホスファターゼ(PTP)が重要である。しかし、PTPの異常が発がんやがんの浸潤・転移にどのように関わっているかについては不明の点が多い。前年度までに、受容体型PTPであるSAP-1の脱リン酸化基質pp90を見出していたが、pp90が炎症性ケモカインの誘導を促進しSAP-1とは拮抗的に作用することで腸管免疫系を制御する可能性を示した。一方、白血病で遺伝子異常が検出されるPTPであるShp2の結合分子SIRP α はマクロファージによる貪食を抑制的に調節している。今年度は、がん細胞株に対する分子標的薬の抗腫瘍効果を抗SIRP α 抗体がさらに増強することを明らかに出来、抗SIRP α 抗体を新たな作用機序を有するがんの分子標的薬としてとして利用できる可能性を示せた。

A. 研究目的

チロシンリン酸化シグナルは、生理的な細胞の増殖・分化・運動の制御に重要なシグナル系であり、一方、がんの発生、浸潤・転移の分子機構にこのシグナル系の異常が深く関与していることが示されている。チロシンリン酸化シグナルの制御には、チロシンキナーゼと共にチロシンホスファターゼ(PTP)が重要であるが、PTPの異常が発がんやがんの浸潤・転移にどのように関わっているかについては未だ不明な点が多い。分担研究者が見出した受容体型PTPであるSAP-1は、ヒト胃がんや大腸がんに高度に発現するPTPであり、大腸がんモデルにおいて、SAP-1ががんの発生を促進的に制御することを見出している。一方、SAP-1は腸上皮細胞の微絨毛に特異的に発現するがその生理機能は未だ不明である。そこで、本研究では、SAP-1の生理機能と発がんにおける役割を明らかにすることを目的とする。前年度までに、SAP-1の脱チロシンリン酸化基質分子として、pp90を見出している。さらに、pp90の組織発現を検討したところ、腸上皮細胞の微絨毛に局在すること、また、pp90の細胞内領域のチロシンリン酸化には、細胞質型チロシンキナーゼが重要であることが分かった。そこで、本年度はさらに、pp90の機能解析を中心に行った。細胞質型PTPであるShp2は増殖因子によるRasの活性化に重要であることが知られており、最近では、Shp2の活性化型遺伝子変異がNoonan症候群と呼ばれる遺伝疾患やそれに随伴するAMLやMDSなどの血液系腫瘍の原因として見出さ

れ注目されている。分担研究者はShp2の結合分子として受容体型分子SIRP α を見出しているが、がんにおける役割は不明である。すでに、SIRP α を高度に発現するヒトメラノーマ細胞のin vitroでの細胞遊走を抗SIRP α 抗体が抑制することを明らかにしている。また、SIRP α はマクロファージに強く発現しており、標的細胞上のリガンド分子であるCD47がSIRP α に結合するとマクロファージによる貪食を負に制御することが知られている。本研究では前年度までに、マウス悪性黒色腫細胞株接種による肺転移モデルにおいて、ADCC活性を有する抗メラノーマ特異的抗体による腫瘍排除を検討したところ、SIRP α 遺伝子破壊(KO)マウスにおいて腫瘍排除が顕著に増強していることを見出した。そこで、本年度はさらに、CD47-SIRP α 系を利用した、新たながん治療法開発の基礎的検討を行った。

B. 研究方法

(1) SAP-1の脱チロシンリン酸化基質分子として前年度までに同定しているpp90の生理機能につき、主に培養細胞系を用いて解析した。また、pp90の細胞内チロシンリン酸化部位への結合分子の探索を行うと共に下流シグナルの解析を行った。

(2) 前年度に引き続き、CD47とSIRP α の結合を阻害する抗SIRP α 抗体、あるいは結合を阻害できない抗SIRP α 抗体のがん細胞株への抗体医薬の増強効果を比較検討した。これらに平行して、SIRP α を高度に発現するマウスあるいはヒトがんの検索を行った。

C. 研究結果

(1) pp90の細胞内領域がチロシンリン酸化され、これにはSH2ドメインを有する細胞質型チロシンキナーゼが結合することを見出した。さらに、pp90の強制発現により、炎症を誘導するシグナル系の活性化やケモカインの発現が誘導されることが明らかとなった。

(2) 血液系のがん細胞株に対する分子標的薬の腫瘍抑制を、CD47とSIRP α の結合を阻害する抗SIRP α 抗体がさらに増強することを明らかに出来た。マウス悪性黒色腫細胞株ではSIRP α の発現が高度であるが、その他の固形がんや血液系のがんでSIRP α の高度な発現を示す細胞株が見出された。

D. 考察

SAP-1はヒト胃がんや大腸がんに高度に発現するPTPである。大腸がんモデルにおいて、SAP-1ががんの発生を促進的に制御することを見出していたが、その分子基盤は不明であった。前年度までに、SAP-1の脱チロシンリン酸化基質として膜貫通型糖化分子であるpp90を同定しており、pp90がSAP-1と同様に腸上皮細胞に高度に発現し微絨毛に局在することも示した。今年度は、pp90がSH2ドメインを有する細胞質型チロシンキナーゼに会合して、炎症惹起に重要なシグナルを活性化することを明らかにした。従って、pp90がSAP-1とは拮抗的に作用することで腸管免疫系を制御する可能性が考えられた。また、CD47とSIRP α の結合を阻害する抗SIRP α 抗体が、血液系のがん細胞株に対する分子標的薬の腫瘍抑制をさらに増強することを明らかに出来た。また、メラノーマ以外のがんにおいてもSIRP α が高度に発現することから、今後、これらのがんにおいても抗SIRP α 抗体の効果を検討する必要性がでてきた。

E. 結論

本研究により、受容体型PTPであるSAP-1の機能には、膜型分子であるpp90が重要である可能性が示された。また、SIRP α 抗体はがんの分子標的薬として利用できる可能性が示された。

G. 研究発表

1. 論文発表

Yamauchi T, Takenaka K, Urata S, Shima T, Kikushige Y, Tokuyama T, Iwamoto C, Nishihara M, Iwasaki H, Miyamoto T, Honma N, Nakao M, Matozaki T, Akashi K. Polymorphic Sirpa is the genetic determinant for NOD-based mouse lines to achieve efficient human cell engraftment. *Blood*. 121:1316-1325, 2013.

Zen K, Guo Y, Bian Z, Lv Z, Zhu D, Matozaki T, Liu Y. Inflammation-induced proteolytic processing of the SIRP α cytoplasmic ITIM in neutrophils propagates a proinflammatory state. *Nat Commun*. 4:2436, 2013.

Yamashita H, Kotani T, Park J, Murata Y, Okazawa H, Ohnishi H, Ku Y, Matozaki T. Role of the protein tyrosine phosphatase Shp2 in homeostasis of the intestinal epithelium. *PloS One*. 9:e92904, 2014.

H. 知的所有権の出願・登録状況

1. 特許取得

なし

2. 実用新案登録

なし

3. その他

なし

研究成果の刊行に関する一覧表

雑誌

発表者氏名	論文タイトル名	発表誌名	巻号	ページ	出版年
Suzuki M, Yamagata K, Shino M, Aikawa Y, Akashi K, Watanabe T, Kitabayashi I.	The nuclear export signal (NES) within CALM is necessary for CALM-AF10-induced leukemia.	Cancer Sci.	105	315-323	2014
Shima H, Yamagata K, Aikawa Y, Shino M, Koseki H, Shimada H, Kitabayashi I.	Bromodomain-PHD finger protein 1 is critical for leukemogenesis associated with MOZ-TIF2 fusion.	Int. J. Hematology	9	21-31	2014
Iwanami A, Gini B, Zanca C, Matsutani T, Assuncao A, Nael A, Dang J, Yang H, Zhu S, Kohyama J, Kitabayashi I, Cavenee WK, Cloughesy TF, Furnari FB, Nakamura M, Toyama Y, Okano H, Mischel PS.	PML mediates glioblastoma resistance to mammalian target of rapamycin (mTOR)-targeted therapies.	Proc Natl Acad Sci U S A.	110	4339-4344	2013
Rokudai S, Laptenko O, Arnal SM, Taya Y, Kitabayashi I, Prives C.	MOZ increases p53 acetylation and premature senescence through its complex formation with PML.	Proc Natl Acad Sci U S A.	110	3895-3900	2013
Haga A, Ogawara Y, Kubota D, Kitabayashi I, Murakami Y, Kondo T.	Interactomic approach for evaluating nucleophosmin-binding proteins as biomarkers for Ewing's sarcoma.	Electrophoresis	34	1670-1678	2013
Shima Y, Honma Y, Kitabayashi I.	Mechanism of PML nuclear body disruption in APL: PML-RAR α inhibits PML oligomerization and its phosphorylation restores PML NBs.	Cancer Res.	73	4278-4288	2013
Shimizu K, Yamagata K, Kurokawa M, Mizutani S, Tsunematsu Y, Kitabayashi I.	Roles of AML1/RUNX1 in T-cell malignancy induced by loss of p53.	Cancer Sci.	103	1033-1038	2013
Yokoyama A, Ficara F, Murphy MJ, Meisel C, Hatanaka C, Kitabayashi I, Cleary ML.	MLL Becomes Functional through Intra-Molecular Interaction Not by Proteolytic Processing.	PLoS One.	8	e73649	2013
Shima T, Miyamoto T, Kikushige Y, Mori Y, Kamezaki K, Takase K, Henzan H, Numata A, Ito Y, Takenaka K, Iwasaki H, Kamimura T, Eto T, Nagafuji K, Teshima T, Kato K, Akashi K	Quantitation of hematogones at the time of engraftment is a useful prognostic indicator in allogeneic hematopoietic stem cell transplantation.	Blood	121	840-848	2013
Kamimura T, Miyamoto T, Yokota N, Takashima S, Chong Y, Ito Y, Akashi K.	Higher incidence of injection site reactions after subcutaneous bortezomib administration on the thigh compared with the abdomen.	Eur J Haematol	90	157-161	2013

Yamauchi T, Takenaka K, Urata S, Shima T, Kikushige Y, Tokuyama T, Iwamoto C, Nishihara M, Iwasaki H, Miyamoto T, Honma N, Nakao M, Matozaki T, Akashi K.	Polymorphic Sirpa is the genetic determinant for NOD-based mouse lines to achieve efficient human cell engraftment.	Blood	121	1316-1325	2013
Fukata M, Ishikawa F, Najima Y, Yamauchi T, Saito Y, Takenaka K, Miyawaki K, Shimazu H, Shimoda K, Kanemaru T, Nakamura K, Odashiro K, Nagafuji K, Harada M, Akashi K.	Contribution of bone marrow-derived hematopoietic stem/progenitor cells to the generation of donor-marker(+) cardiomyocytes in vivo.	PLoS One	8	e62506	2013
Iwamoto C, Takenaka K, Urata S, Yamauchi T, Shima T, Kuriyama T, Daitoku S, Saito Y, Miyamoto T, Iwasaki H, Kitabayashi I, Itoh K, Kishimoto J, Kohda D, Matozaki T, Akashi K.	The BALB/c-specific polymorphic SIRPA enhances its affinity for human CD47, inhibiting phagocytosis against human cells to promote xenogeneic engraftment.	Exp Hematol	42	163-171	2014
Niimi K, Kiyoi H, Ishikawa Y, Hayakawa F, Kurahashi S, Kihara R, Tomita A, Naoe T.	GATA2 zinc finger 2 mutation found in acute myeloid leukemia impairs myeloid differentiation.	Leukemia Research Reports	2	21-25	2013
Hayakawa F, Sugimoto K, Harada Y, Hashimoto N, Ohi N, Kurahashi S, Naoe T.	A novel STAT inhibitor, OPB-31121, has a significant antitumor effect on leukemia with STAT-addictive oncokinasases.	Blood Cancer J	3	e166	2013
Yamaguchi H, Takanashi M, Yoshida N, Ito Y, Kamata R, Fukami K, Yanagihara K, Sakai R.	Saracatinib impairs the peritoneal dissemination of diffuse-type gastric carcinoma cells resistant to Met and fibroblast growth factor receptor inhibitors.	Cancer Sci.	105	528-536	2014
Yamaguchi H, Yoshida N, Takanashi M, Ito Y, Fukami K, Yanagihara K, Yashiro M, Sakai R.	Stromal fibroblasts mediate extracellular matrix remodeling and invasion of scirrhous gastric carcinoma cells.	PLoS One	9	e85485	2014
Miyazawa Y, Uekita T, Ito Y, Seiki M, Yamaguchi H, Sakai R.	CDCP1 regulates the function of MT1-MMP and invadopodia-mediated invasion of cancer cells.	Mol Cancer Res.	11	628-637	2013
Shirakihara T, Kawasaki T, Fukagawa A, Semba K, Sakai R, Miyazono K, Miyazawa K, Saitoh M.	Identification of integrin $\alpha 3$ as a molecular marker of cells undergoing epithelial-mesenchymal transition and of cancer cells with aggressive phenotypes.	Cancer Sci.	104	1189-1197	2013
Kasuga M, Ueki K, Tajima N, Noda M, Ohashi K, Noto H, Goto A, Ogawa W, Sakai R, Tsugane S, Hamajima N, Nakagama H, Tajima K, Miyazono K, Imai K.	Report of the Japan Diabetes Society/Japanese Cancer Association Joint Committee on Diabetes and Cancer.	Cancer Sci.	104	965-976	2013

Uekita T, Fujii S, Miyazawa Y, Hashiguchi A, Abe H, Sakamoto M, Sakai R.	Suppression of autophagy by CUB domain-containing protein 1 signaling is essential for anchorage-independent survival of lung cancer cells.	Cancer Sci.	104	865-870	2013
Zen K, Guo Y, Bian Z, Lv Z, Zhu D, Matozaki T, Liu Y.	Inflammation-induced proteolytic processing of the SIRP α cytoplasmic ITIM in neutrophils propagates a proinflammatory state.	Nat Commun	4	2436	2013
Yamashita H, Kotani T, Park J, Murata Y, Okazawa H, Ohnishi H, Ku Y, Matozaki T.	Role of the protein tyrosine phosphatase Shp2 in homeostasis of the intestinal epithelium.	PloS One	9	e92904	2014

Nuclear export signal within CALM is necessary for CALM-AF10-induced leukemia

Mai Suzuki,¹ Kazutsune Yamagata,¹ Mika Shino,¹ Yukiko Aikawa,¹ Koichi Akashi,² Toshio Watanabe³ and Issay Kitabayashi¹

¹Division of Hematological Malignancy, National Cancer Center Research Institute, Tokyo; ²Department of Medicine and Biosystemic Science, Kyushu University Graduate School of Medical Science, Fukuoka; ³Department of Biological Science, Graduate School of Humanities and Sciences, Nara Women's University, Nara, Japan

Key words

AF10, chromosome translocation, histone modification, leukemia, nuclear export signal

Correspondence

Issay Kitabayashi, Division of Hematological Malignancy, National Cancer Center Research Institute, Tsukiji 5-1-1, Chuo-ku, Tokyo 104-0045, Japan.
Tel: +81-3-3542-2511; Fax: +81-3542-0688;
E-mail: ikitabay@ncc.go.jp

Funding Information

Ministry of Health, Labor, and Welfare. Ministry of Education, Culture, Sports, Science, and Technology. National Cancer Center Research and Development Fund. Naito Foundation. Cosmetology Research Foundation. Nara Women's University Intramural Grant for Project Research.

Received September 16, 2013; Revised December 5, 2013; Accepted December 30, 2013

Cancer Sci 105 (2014) 315–323

doi: 10.1111/cas.12347

The chromosome translocation t(10;11)(p13;q14), found in T-cell acute lymphoblastic leukemia (T-ALL), acute myeloid leukemia (AML) and malignant lymphomas, results in the fusion of the clathrin assembly lymphoid myeloid leukemia protein (CALM) and AF10^(1,2). The CALM-AF10 fusion protein consists of almost all CALM and AF10 proteins, with the exception of one or two plant homeodomain (PHD)^(1,3). AF10, also known as MLLT10, interacts with the transcription factor Ikaros and H3K4me3 through its octapeptide motif-leucine zipper (OM-LZ) region and PHD domains, respectively.^(4–6) In both mice and humans, CALM-AF10 upregulates certain HOXA cluster genes (HOXA5, HOXA7, HOXA9 and HOXA10) and MEIS1.^(7,8) Hoxa5 upregulation, which is critical for CALM-AF10-induced leukemogenesis,^(9,10) is mediated by an interaction between the AF10 OM-LZ region and the histone methyltransferase DOT1L, resulting in H3K79 hypermethylation at the Hoxa5 locus.⁽⁹⁾ These findings suggest that CALM-AF10 might function in the nucleus.

The CALM protein shuttles between the cytoplasm and the nucleus under the control of a CRM1-dependent nuclear export signal (NES).⁽¹¹⁾ In contrast to AF10, which localizes in the nucleus,⁽⁴⁾ CALM-AF10 primarily localizes in the cytoplasm.^(6,9) Other fusion partners of AF10 in acute myeloid and lymphoid leukemias include MLL, DDX3 and HNRNP1.^(12,13)

The CALM-AF10 fusion gene, which results from a t(10;11) translocation, is found in a variety of hematopoietic malignancies. Certain HOXA cluster genes and MEIS1 genes are upregulated in patients and mouse models that express CALM-AF10. Wild-type clathrin assembly lymphoid myeloid leukemia protein (CALM) primarily localizes in a diffuse pattern within the cytoplasm, whereas AF10 localizes in the nucleus; however, it is not clear where CALM-AF10 acts to induce leukemia. To investigate the influence of localization on leukemogenesis involving CALM-AF10, we determined the nuclear export signal (NES) within CALM that is necessary and sufficient for cytoplasmic localization of CALM-AF10. Mutations in the NES eliminated the capacity of CALM-AF10 to immortalize murine bone-marrow cells *in vitro* and to promote development of acute myeloid leukemia in mouse models. Furthermore, a fusion of AF10 with the minimal NES can immortalize bone-marrow cells and induce leukemia in mice. These results suggest that during leukemogenesis, CALM-AF10 plays its critical roles in the cytoplasm.

MLL and hNRNP1 primarily localize in the nucleus,^(14,15) whereas DDX3, like CALM, is mostly distributed throughout the cytoplasm.^(16,17) These observations prompted us to investigate whether CALM-AF10 exerts its function in the nucleus or the cytoplasm. We found that mutant CALM-AF10 lacking the NES localized in the nucleus and lost its ability to induce leukemia in mice. Conversely, a fusion consisting of the minimal NES and AF10 localized in the cytoplasm and induced leukemia. These results indicate that the cytoplasmic location of CALM-AF10 is critical for its role in leukemogenesis.

Materials and Methods

Generation of CALM-AF10 mutant constructs. Plasmid encoding pcDNA3β-FLAG-CALM-AF10 was a gift from Y. Zhang (Department of Biochemistry and Biophysics, University of North Carolina).⁽⁹⁾ Plasmid encoding the NES-deficient mutant FLAG-CALM^{NES4A}-AF10 and FLAG-CALM^{NES4A} were generated by introducing four point mutations into the CALM NES sequence by inverse PCR using a site-specific mutagenesis kit (Toyobo, Osaka, Japan).⁽¹⁸⁾ Specifically, leucine (L)-544, L-547, L-551 and isoleucine (I)-553 in the putative NES sequence within CALM-AF10 were replaced by alanine (A), using the following primers: L544A, 5'-GCAGCCAACCTTGTGG

GCAATCTTGGC-3', and 5'-AGATGAATCCAAGTCATCAGAACTACT-3'; L547A, 5'-GCTGTGGGCAATCTTGGCATCGGAAAT-3', and 5'-GTTGGCTGCAGATGAATCCAAGTCA-3'; L551A, 5'-GCTGGCATCGGAAATGGAACCACTAAG-3', and 5'-ATTGCCACAGCGTTGGCTGCAGAT-3'; I553A, 5'-GCCGAAA TGGAACCACTAAGAATGAT-3', and 5'-GCCAGCATTGCCACAGCGTTGGCT-3'. All mutations were confirmed by DNA sequencing. The AF10 sequence encoding amino acids 81–1027 (mAF10) was amplified by PCR and cloned into pcDNA3 β -FLAG. To generate the fusion of the minimal NES with AF10, NES1 (amino acids 543–554) or NES2 (amino acids 539–558) within CALM was generated by PCR amplification using FLAG-CALM-AF10 as a template, and then cloned into pcDNA3 β -FLAG-mAF10. The pMY-IG-FLAG-CALM-AF10-IRES-GFP, pMY-IG-FLAG-CALM^{NES4A}-AF10-IRES-GFP, pMY-IG-FLAG-mAF10-IRES-GFP and pMY-IG-FLAG-NES2-AF10-IRES-GFP constructs were generated by inserting the corresponding cDNA into the pMY-IG-IRES-GFP vector.

Cell culture and transfection. COS-7 cells were maintained in DMEM supplemented with 10% FBS, 100 U/mL penicillin, 100 μ g/mL streptomycin and 2 mM L-glutamine at 37°C in a humidified 5% CO₂ incubator. COS-7 cells were transfected with pcDNA3 β -FLAG constructs using the Effectene Transfection Reagent (Qiagen, Hilden, Germany).

Immunofluorescence analysis. Forty-eight hours after transfection, COS-7 cells transfected with pcDNA3 β -FLAG constructs were fixed with 3.7% formaldehyde in PBS and examined by immunofluorescence staining with anti-FLAG M2 monoclonal antibody (Sigma-Aldrich, St. Louis, MO, USA), followed by secondary Alexa Fluor 488-conjugated goat anti-mouse IgG (Invitrogen, Carlsbad, CA, USA). Stained cells were mounted in VECTASHIELD mounting medium and observed using a BX50 fluorescence microscope (Olympus, Tokyo, Japan). Cytospins of murine bone-marrow cells transduced with pMY-IG/IRES-GFP viral constructs encoding FLAG-CALM-AF10, FLAG-CALM^{NES4A}-AF10, FLAG-NES2-AF10 or FLAG-mAF10 were fixed with 4% paraformaldehyde and stained with anti-FLAG M2 monoclonal antibody (Sigma-Aldrich) and anti-KMT4/DOT1L polyclonal rabbit antibody (Abcam, Cambridge, MA, USA), followed by secondary Alexa Fluor 568-conjugated goat anti-mouse IgG (Invitrogen) and Alexa Fluor 488-conjugated goat anti-rabbit IgG (Invitrogen), respectively. Stained bone-marrow cells were mounted in VECTASHIELD mounting medium with DAPI (Vector Laboratories, Burlingame, CA, USA) or Prolong Gold (Invitrogen) and observed under a BZ-9000 fluorescence microscope (Keyence Corporation, Osaka, Japan) or a FluoView FV10i confocal laser scanning microscopy (Olympus).

Retroviral infection and bone-marrow transplantation. C57BL/6J mice were purchased from CLEA Japan (Tokyo, Japan). All mouse experiments were approved by the National Cancer Center Animal Ethics Committee and performed in accordance with the institutional guidelines. The pMY-IG/IRES-GFP constructs encoding FLAG-CALM-AF10, FLAG-CALM^{NES4A}-AF10, FLAG-NES2-AF10 or FLAG-mAF10 were transfected into PLAT-E cells using the GeneJuice transfection reagent (Novagen, Nottingham, UK), and retrovirus supernatants were collected 48 h after transfection. c-kit⁺ cells (1×10^5 cells), selected from murine total bone-marrow cells using CD117 MicroBeads (Miltenyi Biotec, Bergisch Gladbach, Germany), were incubated with the retrovirus and RetroNectin (Takara Bio, Madison, WI, USA) for 24 h in StemPro-34 SFM medium (Invitrogen) containing cytokines (20 ng/mL SCF, 10 ng/mL IL-6 and 10 ng/mL IL-3). The transduced donor bone-marrow

cells were then transplanted into lethally irradiated (9.5 Gy) 7–8-week-old female C57BL/6J recipient mice by intravenous injection. For secondary transplants, bone-marrow cells from the primary leukemia mice were intravenously injected into sublethally irradiated (6 Gy) female C57BL/6J mice.

Serial-replating assay. Bone-marrow cells transduced with pMY-IG/IRES-GFP constructs encoding FLAG-CALM-AF10, FLAG-CALM^{NES4A}-AF10, FLAG-NES2-AF10 or FLAG-mAF10 were cultured for 3 days in methylcellulose medium (MethoCult M3234; StemCell Technologies, Vancouver, Canada) supplemented with murine SCF, IL-3 and GM-CSF. The GFP⁺ cells in methylcellulose medium were then sorted using a JSAN cell sorter (Bay Bioscience, Kobe, Japan) and replated every 3–4 days in methylcellulose medium; colonies and cells were counted at each passage. Cells from the second-round and fifth-round colonies were harvested and analyzed by real-time PCR (RT-PCR).

Real time-PCR analysis. Total RNA from replating colonies was purified using an RNeasy Mini Kit (Qiagen). Purified RNA were reverse-transcribed into cDNA using the High Capacity cDNA Reverse Transcription Kit (Applied Biosystems, Foster City, CA, USA). Real-time PCR was performed using the 7500 Fast Real-time PCR System (Applied Biosystems) using the FastStart Universal Probe Master with ROX (Roche, Basel, Switzerland) and the following TaqMan probes (Applied Biosystems): *Hoxa5* (Mm04213381_s1), *Hoxa7* (Mm00657963_m1), *Hoxa9* (Mm00439364_m1), *Hoxa10* (Mm00433966_m1) and *Meis1* (Mm00487664_m1). The relative expression levels of these genes were normalized against the level of *Actb* (Mm00607939_s1).

Flow-cytometry analysis. Bone-marrow cells from leukemic mice were pre-incubated with rat IgG (Sigma-Aldrich), and then incubated on ice with the appropriate staining reagents: anti-CD115(CSF1R)-PE (eBioscience, San Diego, CA, USA), anti-Mac-1(M1/70)-PE-Cy7 (eBioscience), anti-Gr-1(RB6-8C5)-APC (BD Pharmingen, San Diego, CA, USA) and anti-c-Kit(2B8)-APC-eF780 (eBioscience). FACS analysis and cell sorting were performed using the JSAN cell sorter and the results were analyzed using the FLOWJO software (Tree Star, Stanford, CA, USA).

Results

The nuclear export signal within CALM is required for cytoplasmic localization of CALM-AF10. To investigate the role of subcellular localization of CALM-AF10 in leukemogenesis, we focused on the NES within the CALM portion of the fusion protein (amino acids 543–554 of CALM).⁽⁹⁾ We generated NES-deficient mutants CALM^{NES4A}-AF10 and CALM^{NES4A}, in which leucine-544, leucine-547, leucine-551 and isoleucine-553 in the putative NES region within CALM were substituted with alanines (NES4A) (Fig. 1a). Expression vectors for FLAG-tagged CALM-AF10, CALM, CALM^{NES4A}-AF10, CALM^{NES4A} and mAF10 (the AF10 portion of CALM-AF10) were transiently transfected into COS-7 cells. Immunofluorescence analysis revealed that CALM and CALM-AF10 primarily localized in the cytoplasm, whereas mAF10 and the NES mutants CALM^{NES4A}-AF10 and CALM^{NES4A} localized in the nucleus (Fig. 1b,c).

To determine the minimal NES, two sequences, NES1 (aa. 543–554) and NES2 (aa. 539–558), were fused to AF10 (Fig. 1a,b). As with mAF10, NES1-AF10 was in the nucleus; by contrast, NES2-AF10 was in the cytoplasm (Fig. 1d). The same results were obtained when these fusion proteins were transduced into murine hematopoietic progenitor cells by retro-

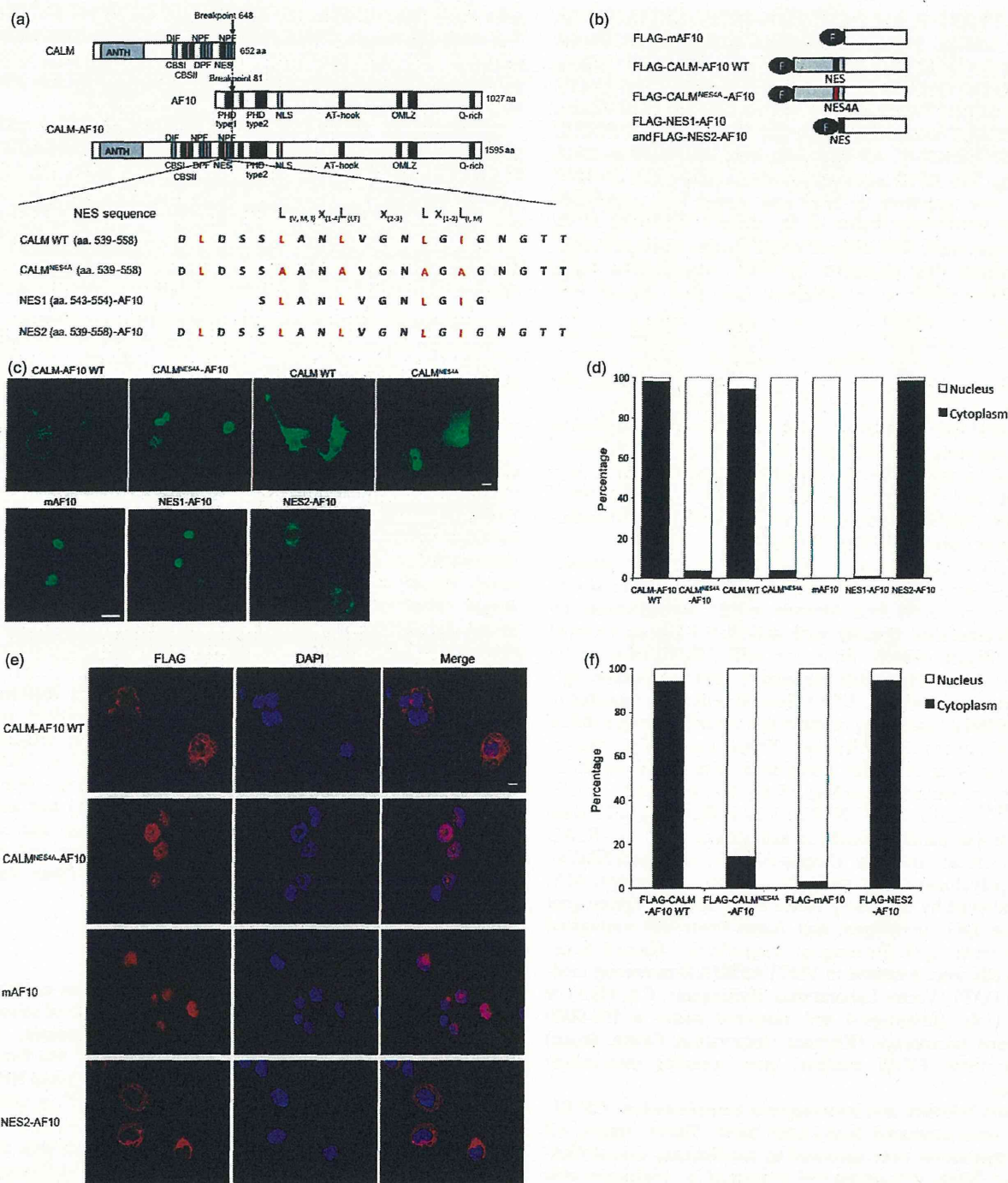


Fig. 1. The NES region within clathrin assembly lymphoid myeloid leukemia protein (CALM) is necessary for cytoplasmic localization. (a) Schematic representations of CALM, AF10, CALM-AF10 and mutant proteins. FLAG-CALM^{NES4A}-AF10 and FLAG-CALM^{NES4A} were generated by alanine substitution of three leucine residues and one isoleucine residue in the putative CALM NES (red). FLAG-NES1-AF10 and FLAG-NES2-AF10 mutants were constructed by fusion of the NES sequences of CALM to the AF10 portion of CALM-AF10. (b) Diagrams of the plasmid constructs used in transfection experiments. (c) Subcellular distribution of CALM-AF10 and the NES point mutations FLAG-CALM-AF10, FLAG-CALM, FLAG-CALM^{NES4A}-AF10, FLAG-CALM^{NES4A}, FLAG-mAF10, FLAG-NES1-AF10, FLAG-NES2-AF10 and FLAG-mAF10 in COS-7 cells. Transfected cells were stained with anti-FLAG antibody (green) and observed by fluorescence microscopy. (d) Population of cells expressing transduced genes in the nucleus and cytoplasm shown in (c). (e) Subcellular distribution of CALM-AF10 and NES mutation proteins in murine bone-marrow cells. Transduced cells were stained with anti-FLAG antibody (red) and observed by fluorescence microscopy. (f) Population of cells expressing transduced genes in the nucleus and the cytoplasm shown in (e). Nuclei were stained with DAPI (blue) and observed by fluorescence microscopy. The scale bar represents 20 μ m in (c) and 10 μ m in (e). ANTH, AP180 N-terminal homology domain binding phosphatidylinositol 4,5-bisphosphate (PIP₂); DIF and DPF, motifs interacts with AP-2; NPF, a motif interacts with the EH (Eps15 homology) domain; CBS-I and -II, putative type I and II clathrin-binding sequences; NES, nuclear export signal; PHD Type1 and 2, plant homeodomain zinc finger domains; NLS, nuclear localization signal; AT-hook, DNA-binding protein motif; OMLZ, octapeptide motif-leucine zipper domain; Q-rich, glutamine-rich region.

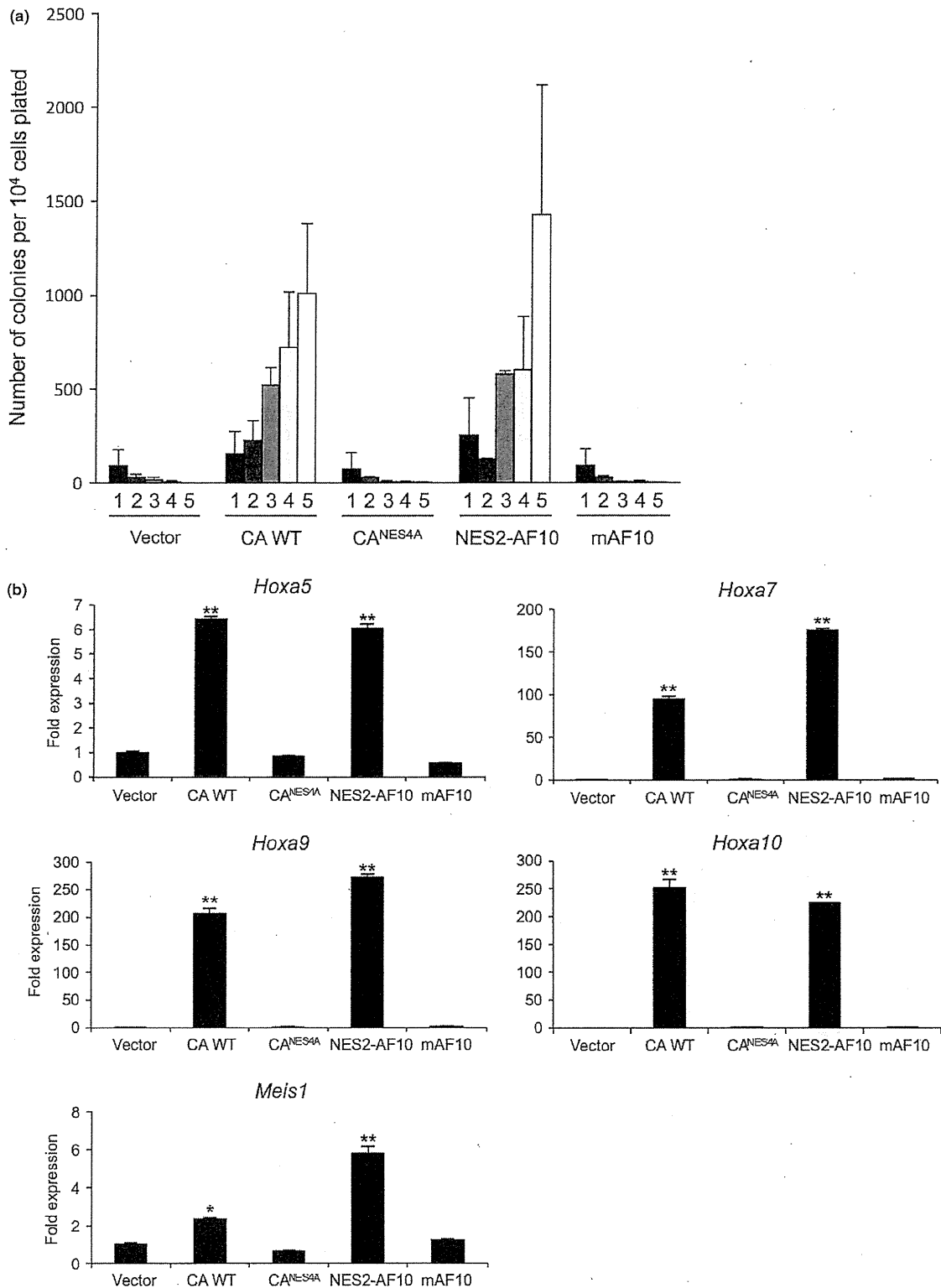


Fig. 2. The nuclear export signal within clathrin assembly lymphoid myeloid leukemia protein (CALM) is critical for *in vitro* immortalization of cells by CALM-AF10. (a) Serial colony-replating assays of murine bone-marrow cells transduced with FLAG-tagged wild-type and mutant CALM-AF10. In each round of replating, 3×10^4 transduced bone-marrow cells were plated. Bars represent the numbers of colonies. (b) *Hoxa* cluster and *Meis1* expression in cells transduced with wild-type or mutant CALM-AF10. RNA transcripts were analyzed by real-time PCR of murine bone-marrow cells transduced with wild-type and mutant CALM-AF10 *in vitro*. Expression levels of *Hoxa5*, *Hoxa7*, *Hoxa9*, *Hoxa10* and *Meis1* were normalized against *Actb* expression and compared with the levels in vector-transfected whole bone-marrow cells. Data are shown as means \pm SEM from three independent samples. * $P < 0.05$; ** $P < 0.01$. (vs normal bone-marrow cells). CA WT, wild-type CALM-AF10.

viral infection (Fig. 1e). These results indicate that NES1 is not sufficient, but its flanking regions including leucine-540 are necessary for cytoplasmic localization of CALM-AF10. Thus, we concluded that the NES2 region is the minimal NES that mediates cytoplasmic localization of CALM-AF10.

The nuclear export signal within CALM is necessary for CALM-AF10-induced immortalization of cells *in vitro*. We next investigated whether the NES within CALM-AF10 is required for leukemogenesis. To this end, primary murine bone-marrow stem/progenitor cells (HSPC) were infected with retrovirus encoding CALM-AF10, CALM^{NES4A}-AF10, NES2-AF10 and mAF10. Serial-replating assays revealed that both CALM-AF10 and NES2-AF10 immortalized HSPC, and that the cells formed colonies for at least five rounds of replating (Fig. 2a). By contrast, neither mAF10 nor CALM^{NES4A}-AF10, which lacks a functional CALM NES, could immortalize cells. Transduced cells with elevated colony-forming abilities also exhib-

ited upregulation of the *Hoxa* cluster (*Hoxa5*, *Hoxa7*, *Hoxa9* and *Hoxa10*) and *Meis1* genes (Fig. 2b)^(7,9). These results indicated that the CALM NES is necessary for CALM-AF10 to immortalize hematopoietic stem/progenitor cells.

The nuclear export signal within CALM-AF10 is necessary to induce leukemia *in vivo*. To determine whether CALM-AF10 and NES2-AF10 can induce leukemia in mice, we injected bone-marrow progenitor cells transduced with CALM-AF10 and NES2-AF10 into lethally irradiated mice. Seven out of eight mice transplanted with cells expressing CALM-AF10 developed leukemia within 6 months after transplantation (Fig. 3a), and all mice transplanted with cells expressing NES2-AF10 developed leukemia within 3 months after transplantation. When cells prepared from bone marrow of these leukemic mice were transplanted into secondary recipient mice, all recipients promptly developed leukemia (medians: CALM-AF10 donors, 21 days [$n = 4$]; NES2-AF10 donors,

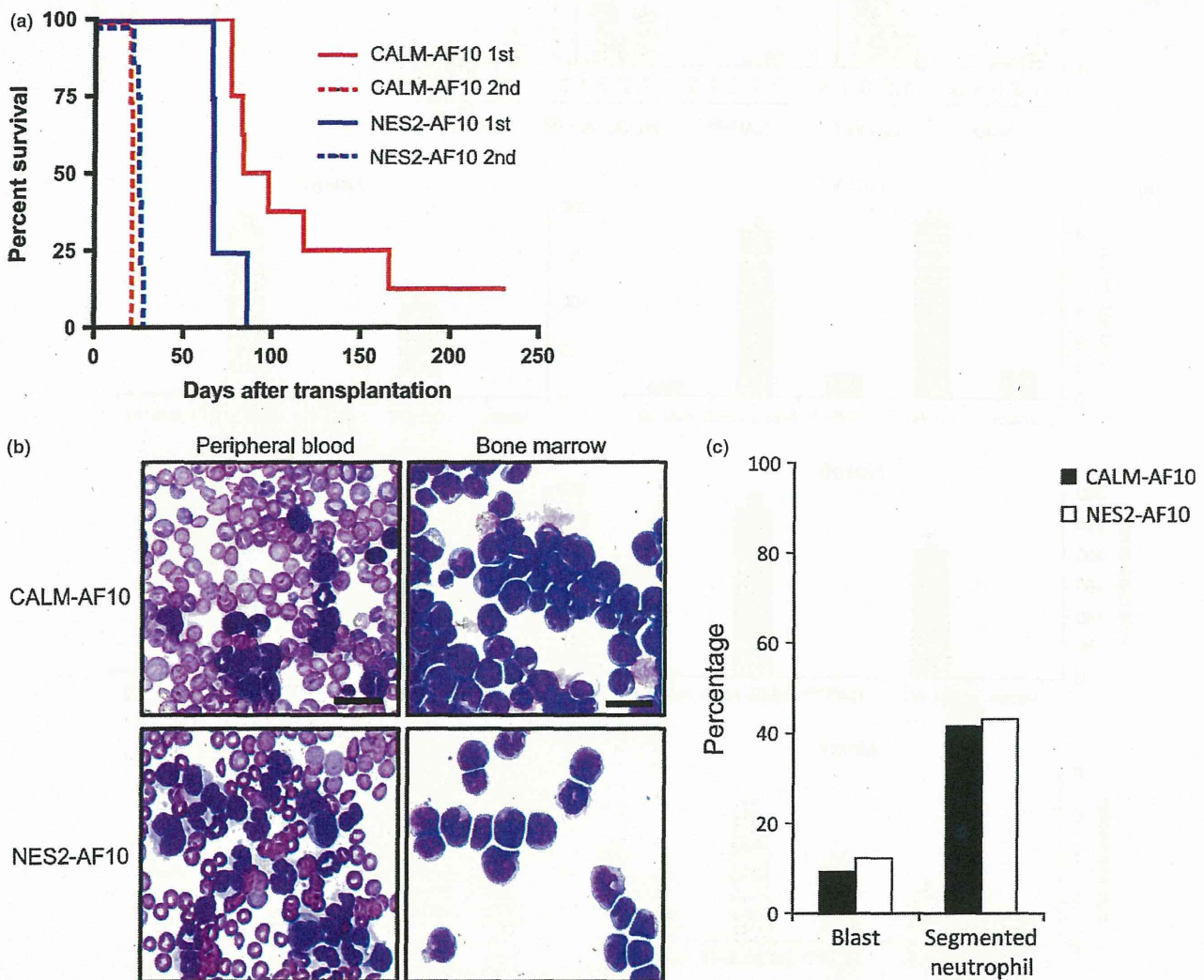


Fig. 3. The nuclear export signal within clathrin assembly lymphoid myeloid leukemia protein (CALM) is sufficient for leukemic transformation by CALM-AF10. (a) Survival of mice injected with murine bone-marrow cells transduced with FLAG-CALM-AF10 or FLAG-NES2-AF10. The leukemia-free survivals of the mice were analyzed. CALM-AF10 primary transplantation, $n = 8$; CALM-AF10 secondary transplantation, $n = 4$; NES2-AF10 primary transplantation, $n = 4$; NES2-AF10 secondary transplantation, $n = 9$. (b) Peripheral blood smears and bone-marrow cytopsins were stained with May-Giemsa from CALM-AF10-transduced or NES2-AF10-transduced bone-marrow cells. Original magnification is 400 \times . (c) Population of blasts and segmented neutrophils in bone-marrow cells shown in (b). The scale bars represent 20 μ m.

25 days [$n = 9$]). Morphological analysis revealed large populations of blast cells in leukemic mice receiving cells transduced with either CALM-AF10 or NES2-AF10 (Fig. 3b, c). Flow cytometry analysis showed that cells expressing CALM-AF10 and NES2-AF10 in the bone marrow cells of primary recipient mice were Mac1⁺, CSF1R⁺ and c-kit⁺ (Fig. 4a).

Moreover, as shown in Figure 4b, *Hoxa5*, *Hoxa7*, *Hoxa9*, *Hoxa10* and *Meis1* expression levels were upregulated in cells expressing CALM-AF10 and NES2-AF10 compared with normal bone marrow cells, although upregulation of *Hoxa5* and *Meis1* in primary recipient mice harboring NES2-AF10 was not significant ($P = 0.084$ and $P = 0.093$, respectively). These

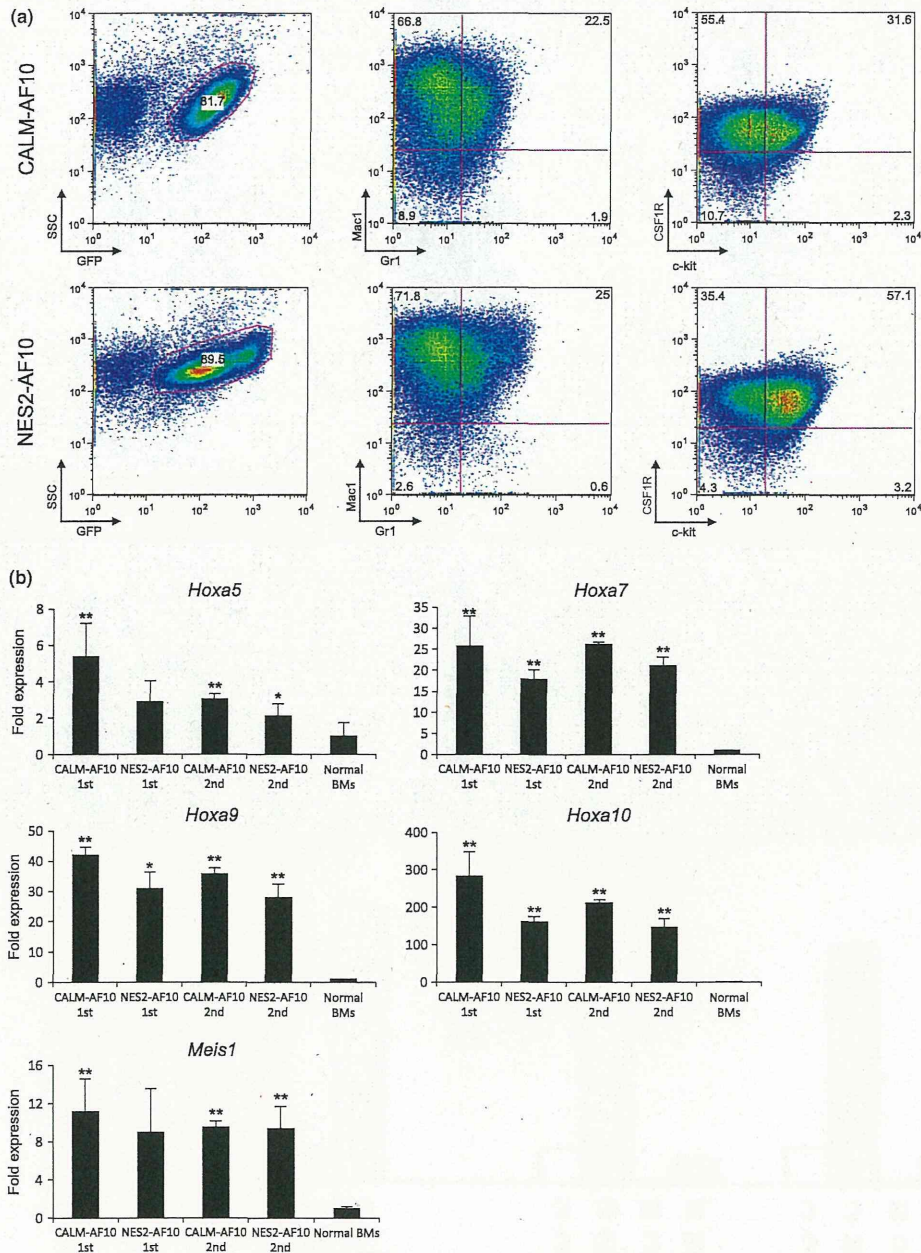


Fig. 4. Characterization of leukemic cells *in vivo*. (a) Flow cytometric analysis of leukemic cells. Murine bone-marrow cells were prepared from mice that developed leukemia after receiving transplantation of tumor cells transduced with CALM-AF10 or NES2-AF10, and were co-stained for Gr-1, Mac-1, colony stimulating factor 1 receptor (CSF1R) and c-kit; data are representative of CALM-AF10 primary transplantation ($n = 3$) and NES2-AF10 primary transplantation ($n = 3$). (b) *Hoxa* cluster and *Meis1* expression in mice receiving cells transduced with wild-type and mutant CALM-AF10. RNA transcripts were analyzed by real-time PCR of bone-marrow cells in mice that developed leukemia after CALM-AF10 and NES2-AF10 bone-marrow transplantation. Expression levels of *Hoxa5*, *Hoxa7*, *Hoxa9*, *Hoxa10* and *Meis1* were normalized against *Actb* and compared with wild-type whole bone marrow. Data are shown as means \pm SEM from three independent leukemic mice. * $P < 0.05$; ** $P < 0.01$ (vs normal bone-marrow cells).

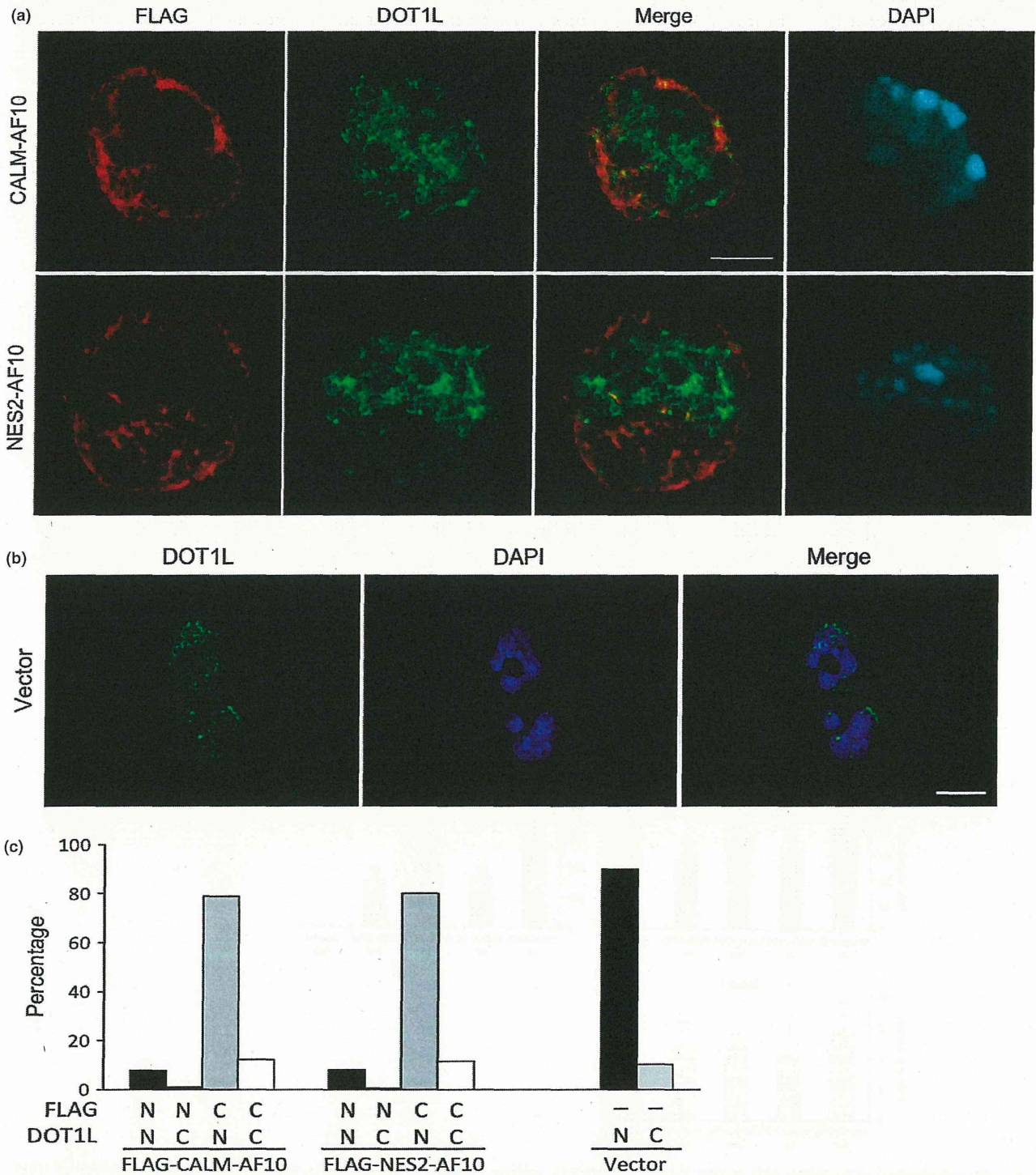


Fig. 5. Dot1L mainly localizes in the nucleus in CALM-AF10-induced or NES2-AF10-induced leukemic cells. (a) Subcellular distribution of endogenous Dot1L in CALM-AF10-induced or NES2-AF10-induced leukemic cells. Cytoplasm of the cells was stained with anti-FLAG antibody (red), anti-DOT1L antibody (green) and DAPI (blue) and observed by confocal laser scanning microscopy. Note that GFP expression was not detected in the condition. (b) Subcellular distribution of endogenous Dot1L in the control vector-infected murine using fluorescence microscopy. (c) Population of leukemia cells expressing DOT1L and CALM-AF10 or FLAG-NES2-AF10 in the nucleus and the cytoplasm shown in (a) and (b). The scale bar represents 5 μm in (a) and 10 μm in (b).

data demonstrate that the NES within CALM-AF10 is a critical element for induction of leukemia.

It has been reported that CALM-AF10 interacts with the histone methyltransferase DOT1L to mediate H3K79 hypermethylation at the *Hoxa5* locus.⁽⁹⁾ To determine whether Dot1L colocalizes with CALM-AF10 and NES2-AF10 in the leukemia cells, we performed immunofluorescence analysis. Dot1L mainly localized in the nucleus while CALM-AF10 and NES2-AF10 mainly localized in the cytoplasm (Fig. 5a,b). Dot1L partially colocalized with both CALM-AF10 and NES2-AF10, but neither CALM-AF10 nor NES2-AF10 altered the localization of Dot1L (Fig. 5a).

Discussion

AF10 and CALM localize diffusely in the nucleus and cytoplasm, respectively, whereas CALM-AF10 primarily localizes in cytoplasmic speckle domains (see Fig. 1c,d). The fact that CALM-AF10 regulates histone methylation at the *Hoxa5* locus suggests that CALM-AF10 is likely to function in the nucleus.⁽⁹⁾ However, the results described here indicate that the CALM NES is essential for CALM-AF10-induced leukemogenesis, suggesting that cytoplasmic localization (or shuttling between nucleus and cytoplasm) is critical for the function of CALM-AF10. During the preparation of the manuscript, another group reported similar findings,⁽¹⁹⁾ indicating that the results are reproducible and the conclusions can be validated using alternative experimental systems.

The molecular mechanism by which CALM-AF10 exerts its function in the cytoplasm remains unclear, but two possibilities are consistent with the existing data: CALM-AF10 may affect cytoplasmic signaling pathways that regulate expression of its target genes, including *HoxA* cluster genes; alternatively, CALM-AF10 may affect the functions of transcriptional regulators by changing their localization from the nucleus to the cytoplasm. DOT1L, a candidate mediator of CALM-AF10-induced leukemia, interacts with AF10 and induces H3K79 hypermethylation at *Hoxa5*.⁽⁹⁾ However, our present data suggest that CALM-AF10 and NES2-AF10 did not affect the localization of Dot1L (see Fig. 5a). It is possible that CALM-AF10 squelches DOT1L inhibitors by exporting them to the cytoplasm.

CALM plays an important role in clathrin-mediated endocytosis.^(17,20,21) It and other endocytosis-related genes, such as

EPS15, EEN, CLTC and HIP1, are involved in multiple types of leukemia-associated chromosomal translocations (e.g. MLL-CALM, MLL-EPS15, MLL-EEN, CLTC-ALK and HIP1-PDGFR),^(22–26) suggesting that these leukemia-associated fusions might affect endocytosis in a manner that contributes to leukemogenesis. However, recent reports have shown that the clathrin-binding domain of CALM is not essential for CALM-AF10-mediated leukemogenesis.^(27,28) Here, we show that nuclear export of CAL-AF10 is critical for the leukemogenesis. Because the endocytosis-related proteins mentioned above are also exported from the nucleus to the cytoplasm, as in the case of CALM,^(11,23,29) it is possible that changes in the localization of fusions involving endocytosis-related proteins have some shared consequence that is important for leukemogenesis.

Molecular exchange between the nucleus and cytoplasm takes place through nuclear pore complexes (NPC). Fusion proteins containing NUP98 and NUP214, which are components of the NPC, have been found in AML and T-ALL;^(30,31) as in cells expressing CALM-AF10, a set of *Hoxa* and *Meis1* genes are upregulated in leukemia cells expressing these NUP98 fusions and NUP214 fusions.^(32,33) In addition, the NPC-component fusions interact with CRM1, the major receptor for the nuclear export of protein.^(33,34) These observations suggest that alteration of the localization of certain factors by NUP98 fusions and NUP214 fusions might be important for leukemogenesis, and that a common mechanism may underlie leukemias induced by CALM and NUP fusions.

Acknowledgments

We thank Dr Y. Zhang for pcDNA3β-FLAG-CALM-AF10 plasmid. This work was supported in part by Grants-in-Aid for Scientific Research from the Ministry of Health, Labor, and Welfare and from the Ministry of Education, Culture, Sports, Science, and Technology; the National Cancer Center Research and Development Fund; the Naito Foundation; Cosmetology Research Foundation; and Nara Women's University Intramural Grant for Project Research. MS is a Research Fellow for Young Scientist of Japan Society for the Promotion of Science.

Disclosure Statement

The authors have no conflict of interest.

References

- Dreyling MH, Martinez-Climent JA, Zheng M, Mao J, Rowley JD, Bohlander SK. The t(10;11)(p13;q14) in the U937 cell line results in the fusion of the AF10 gene and CALM, encoding a new member of the AP-3 clathrin assembly protein family. *Proc Natl Acad Sci USA* 1996; **93**: 4804–9.
- Bohlander SK, Muschinsky V, Schrader K *et al*. Molecular analysis of the CALM/AF10 fusion: identical rearrangements in acute myeloid leukemia, acute lymphoblastic leukemia and malignant lymphoma patients. *Leukemia* 2000; **14**: 93–9.
- Narita M, Shimizu K, Hayashi Y *et al*. Consistent detection of CALM-AF10 chimaeric transcripts in haematological malignancies with t(10;11)(p13;q14) and identification of novel transcripts. *Br J Haematol* 1999; **105**: 928–37.
- Linder B, Newman R, Jones LK *et al*. Biochemical analyses of the AF10 protein: the extended LAP/PHD-finger mediates oligomerisation. *J Mol Biol* 2000; **299**: 369–78.
- Wysocka J, Swigut T, Xiao H *et al*. A PHD finger of NURF couples histone H3 lysine 4 trimethylation with chromatin remodelling. *Nature* 2006; **442**: 86–90.
- Greif PA, Tizazu B, Krause A, Kremmer E, Bohlander SK. The leukemogenic CALM/AF10 fusion protein alters the subcellular localization of the lymphoid regulator Ikaros. *Oncogene* 2008; **27**: 2886–96.
- Caudell D, Zhang Z, Chung YJ, Aplon PD. Expression of a CALM-AF10 fusion gene leads to Hoxa cluster overexpression and acute leukemia in transgenic mice. *Cancer Res* 2007; **67**: 8022–31.
- Mulaw MA, Krause A, Deshpande AJ *et al*. CALM/AF10-positive leukemias show upregulation of genes involved in chromatin assembly and DNA repair processes and of genes adjacent to the breakpoint at 10p12. *Leukemia* 2012; **26**: 1012–9.
- Okada Y, Jiang Q, Lemieux M, Jeannotte L, Su L, Zhang Y. Leukaemic transformation by CALM-AF10 involves upregulation of *Hoxa5* by hDOT1L. *Nat Cell Biol* 2006; **8**: 1017–24.
- Chen L, Deshpande AJ, Banka D *et al*. Abrogation of MLL-AF10 and CALM-AF10-mediated transformation through genetic inactivation or pharmacological inhibition of the H3K79 methyltransferase Dot1l. *Leukemia* 2013; **27**: 813–22.
- Vecchi M, Polo S, Poupon V, van de Loo JW, Benmerah A, Di Fiore PP. Nucleocytoplasmic shuttling of endocytic proteins. *J Cell Biol* 2001; **153**: 1511–7.
- Borkhardt A, Haas OA, Strobl W *et al*. A novel type of MLL/AF10 fusion transcript in a child with acute megakaryocytic leukemia (Aml-M7). *Leukemia* 1995; **9**: 1796–7.
- Brandimarte L, Pierini V, Di Giacomo D *et al*. New MLLT10 gene recombinations in pediatric T-acute lymphoblastic leukemia. *Blood* 2013; **121**: 5064–7.

- 14 Lee JW, Liao PC, Young KC *et al.* Identification of hnRNP1, NF45, and C14orf166 as novel host interacting partners of the mature hepatitis C virus core protein. *J Proteome Res* 2011; **10**: 4522–34.
- 15 Ennas MG, Sorio C, Greim R *et al.* The human ALL-1/MLL/HRX antigen is predominantly localized in the nucleus of resting and proliferating peripheral blood mononuclear cells. *Cancer Res* 1997; **57**: 2035–41.
- 16 Yedavalli VSRK, Neuveut C, Chi YH, Kleiman L, Jeang KT. Requirement of DDX3 DEAD box RNA helicase for HIV-1 Rev-RRE export function. *Cell* 2004; **119**: 381–92.
- 17 Tebar F, Bohlander SK, Sorkin A. Clathrin assembly lymphoid leukemia (CALM) protein: localization in endocytic-coated pits, interactions with clathrin, and the impact of overexpression on clathrin-mediated traffic. *Mol Biol Cell* 1999; **10**: 2687–702.
- 18 Takagi M, Nishioka M, Kakihara H *et al.* Characterization of DNA polymerase from *Pyrococcus* sp. strain KOD1 and its application to PCR. *Appl Environ Microbiol* 1997; **63**: 4504–10.
- 19 Conway AE, Scotland PB, Lavau CP, Wechsler DS. A CALM-derived nuclear export signal is essential for CALM-AF10-mediated leukemogenesis. *Blood* 2013; **121**: 4758–68.
- 20 Ford MGJ, Pearse BMF, Higgins MK *et al.* Simultaneous binding of PtdIns (4,5)P-2 and clathrin by AP180 in the nucleation of clathrin lattices on membranes. *Science* 2001; **291**: 1051–5.
- 21 Meyerholz A, Hinrichsen L, Groos S, Esk PC, Brandes G, Ungewickell EJ. Effect of clathrin assembly lymphoid leukemia protein depletion on clathrin coat formation. *Traffic* 2005; **6**: 1225–34.
- 22 Bernard OA, Mauchauffe M, Mecucci C, Vandenberghe H, Berger R. A novel gene, Af-1p, fused to Hrx in T(1,11)(P32, Q23), is not related to Af-4, Af-9 nor Enl. *Oncogene* 1994; **9**: 1039–45.
- 23 So CW, So CKC, Cheung N, Chew SL, Sham MH, Chan LC. The interaction between EEN and Abi-1, two MLL fusion partners, and synaptojanin and dynamin: implications for leukaemogenesis. *Leukemia* 2000; **14**: 594–601.
- 24 Bridge JA, Kanamori M, Ma ZG *et al.* Fusion of the ALK gene to the clathrin heavy chain gene, CLTC, in inflammatory myofibroblastic tumor. *Am J Pathol* 2001; **159**: 411–5.
- 25 Wechsler DS, Engstrom LD, Alexander BM, Motto DG, Roulston D. A novel chromosomal inversion at 11q23 in infant acute myeloid leukemia fuses MLL to CALM, a gene that encodes a clathrin assembly protein. *Genes Chromosomes Cancer* 2003; **36**: 26–36.
- 26 Ross TS, Bernard OA, Berger R, Gilliland DG. Fusion of Huntingtin interacting protein 1 to platelet-derived growth factor beta receptor (PDGF beta R) in chronic myelomonocytic leukemia with t(5;7)(q33;q11.2). *Blood* 1998; **91**: 4419–26.
- 27 Deshpande AJ, Rouhi A, Lin Y *et al.* The clathrin-binding domain of CALM and the OM-LZ domain of AF10 are sufficient to induce acute myeloid leukemia in mice. *Leukemia* 2011; **25**: 1718–27.
- 28 Stoddart A, Tennant TR, Fernald AA, Anastasi J, Brodsky FM, Le Beau MM. The clathrin-binding domain of CALM-AF10 alters the phenotype of myeloid neoplasms in mice. *Oncogene* 2012; **31**: 494–506.
- 29 Engqvist-Goldstein AEY, Kessels MM, Chopra VS, Hayden MR, Drubin DG. An actin-binding protein of the Sla2/Huntingtin interacting protein 1 family is a novel component of clathrin-coated pits and vesicles. *J Cell Biol* 1999; **147**: 1503–18.
- 30 von Lindern M, Breems D, van Baal S, Adriaansen H, Grosveld G. Characterization of the translocation breakpoint sequences of two DEK-CAN fusion genes present in t(6;9) acute myeloid leukemia and a SET-CAN fusion gene found in a case of acute undifferentiated leukemia. *Genes Chromosomes Cancer* 1992; **5**: 227–34.
- 31 Nakamura T, Largaespada DA, Lee MP *et al.* Fusion of the nucleoporin gene NUP98 to HOXA9 by the chromosome translocation t(7;11)(p15;p15) in human myeloid leukaemia. *Nat Genet* 1996; **12**: 154–8.
- 32 Nakamura T. NUP98 fusion in human leukemia: dysregulation of the nuclear pore and homeodomain proteins. *Int J Hematol* 2005; **82**: 21–7.
- 33 Van Vlierberghe P, van Grotel M, Tchinda J *et al.* The recurrent SET-NUP214 fusion as a new HOXA activation mechanism in pediatric T-cell acute lymphoblastic leukemia. *Blood* 2008; **111**: 4668–80.
- 34 Takeda A, Sarma NJ, Abdul-Nabi AM, Yaseen NR. Inhibition of CRM1-mediated nuclear export of transcription factors by leukemogenic NUP98 fusion proteins. *J Biol Chem* 2010; **285**: 16248–57.

Bromodomain-PHD finger protein 1 is critical for leukemogenesis associated with MOZ–TIF2 fusion

Haruko Shima · Kazutsune Yamagata ·
Yukiko Aikawa · Mika Shino · Haruhiko Koseki ·
Hiroyuki Shimada · Issay Kitabayashi

Received: 29 June 2013 / Revised: 3 November 2013 / Accepted: 5 November 2013 / Published online: 21 November 2013
© The Japanese Society of Hematology 2013

Abstract Chromosomal translocations that involve the monocytic leukemia zinc finger (MOZ) gene are typically associated with human acute myeloid leukemia (AML) and often predict a poor prognosis. Overexpression of HOXA9, HOXA10, and MEIS1 was observed in AML patients with MOZ fusions. To assess the functional role of HOX upregulation in leukemogenesis by MOZ–TIF2, we focused on bromodomain-PHD finger protein 1 (BRPF1), a component of the MOZ complex that carries out histone acetylation for generating and maintaining proper epigenetic programs in hematopoietic cells. Immunoprecipitation analysis showed that MOZ–TIF2 forms a stable complex with BRPF1, and chromatin immunoprecipitation analysis showed that MOZ–TIF2 and BRPF1 interact with HOX genes in MOZ–TIF2-induced AML cells. Depletion of BRPF1 decreased the MOZ localization on HOX genes, resulting in loss of transformation ability induced by MOZ–TIF2. Furthermore, mutant MOZ–TIF2 engineered to lack histone acetyltransferase activity was incapable of deregulating HOX genes as well as initiating leukemia. These data indicate that MOZ–TIF2/BRPF1 complex

upregulates HOX genes mediated by MOZ-dependent histone acetylation, leading to the development of leukemia. We suggest that activation of BRPF1/HOX pathway through MOZ HAT activity is critical for MOZ–TIF2 to induce AML.

Keywords MOZ–TIF2 · BRPF1 · HOX genes · AML

Introduction

Monocytic leukemia zinc finger protein (MOZ) is a MYST (MOZ, Ybf2 (Sas3), Sas2, Tip60)-type histone acetyltransferase (HAT), and interacts with AML1, PU.1 or p53 to activate transcriptions of their target genes [1–3]. While MOZ plays a crucial role in the maintenance of normal hematopoietic stem cells [4], MOZ is also involved in chromosomal translocations such as t(8;16)(p11;p13), t(8;22)(p11;q13) and inv(8)(p11;q13), resulting in fusions of MOZ–CBP, MOZ–p300 and MOZ–TIF2, respectively, which are associated with acute myelomonocytic leukemia [5–8]. MOZ-related translocations are observed in approximately 1–6.5 % of AML, and indicate poor prognosis [9, 10]. We have previously shown that upregulation of M-CSFR (CSF1R) mediated by PU.1 is crucial for the maintenance of AML stem cells in MOZ–TIF2 leukemia [2]. However, although deletion of *CSF1R* delayed the onset of MOZ–TIF2 leukemia in vivo, approximately half of the mice transplanted with *CSF1R*-deleted, MOZ–TIF2-transduced cells developed leukemia in the long term. This may suggest the presence of another pathway involved in the generation of MOZ–TIF2 leukemia.

To pursue other pathways independent of PU.1/M-CSFR pathway, we focused on *HOX* genes. Enforced

H. Shima · K. Yamagata · Y. Aikawa · M. Shino ·
I. Kitabayashi (✉)
Division of Hematological Malignancy, National Cancer Center
Research Institute, 5-1-1 Tsukiji, Chuo-ku, Tokyo 104-0045,
Japan
e-mail: ikitabay@ncc.go.jp

H. Shima · H. Shimada
Department of Pediatrics, Keio University School of Medicine,
Tokyo, Japan

H. Koseki
Department of Developmental Genetics, RIKEN Research
Center for Allergy and Immunology, RIKEN Yokohama
Institute, Yokohama, Japan

expression of *HOXA9* or *HOXA10* immortalizes bone marrow (BM) progenitors in vitro [11, 12]. However, *HOXA9* or *HOXA10* overexpressed cells require relatively long latency period to induce leukemia in recipient mice. This may suggest that another complementing mutation would be needed for dominant outgrowth of transplanted cell [13, 14].

HOX genes are upregulated in BM samples of patients with MOZ-related leukemias as well as in BM cells of MOZ-TIF2-induced AML mouse model [2, 15]. MOZ forms complex with ING5 (inhibitor of growth 5), EAF6 (homolog of Esal-associated factor 6), and BRPF1/2/3 (bromodomain-PHD finger protein 1, 2 or 3), and MOZ is the catalytic component of this HAT complex [9]. Recently, it was reported that BRPF1, a component of the HAT complex is required for the maintenance of *HOX* genes expression [16, 17]. Because HAT domain is intact in most of the fusions and sufficient for forming HAT complex [9], MOZ fusions may also form complex and deregulate *HOX* genes mediated by BRPF1. This study was performed to determine the role of BRPF1 in the regulation of *HOX* genes, and in the generation of MOZ-TIF2 leukemia.

Methods

Mice

C57/BL6 mice were purchased from CREA Japan. Mouse experiments were performed in a specific pathogen-free environment at the National Cancer Center animal facility according to institutional guidelines with approval of the National Cancer Center Animal Ethics Committee.

Plasmids

MOZ and MOZ-TIF2 plasmids used here were described previously [1, 2]. Human BRPF1 cDNA was purchased from Openbiosystems and inserted into MSCV-neo vector. Human *HOXA9* cDNA was isolated by cloning K562 cells and inserted into MSCV-neo vector. Deletion mutants of MOZ-TIF2 and BRPF1 and point mutants of MOZ were constructed by ligation of the cDNA fragments made by restriction enzymes and PCRs.

Retrovirus transduction and AML mouse model

Plasmid DNA was transfected into PlatE packaging cells using the FuGENE 6 reagent (Roche Diagnostics), and supernatants containing retrovirus were collected 48 h after transfection. c-kit⁺ progenitors were obtained from BM mononuclear cells using anti-CD117 beads (Miltenyi Biotec.) and incubated with retrovirus in a retrofectin (Takara

Fig. 1 Effects of *Brpf1* knockdown on MOZ-TIF2 leukemic cells in vitro. **a** HA-tagged wild-type MOZ-TIF2 was cotransfected into 293FT cells together with FLAG-tagged WT BRPF1, deletion 1–222 (Δ 1–222) BRPF1, or empty vector. Immunoprecipitates with anti-FLAG antibody (M2 IP) or cell lysates (Extracts) were subjected to immunoblotting with anti-HA or anti-FLAG antibodies. Δ 1–222 BRPF1 lost its ability to coprecipitate with MOZ-TIF2. **b** Efficiency of *Brpf1* knockdown by *Brpf1* shRNA on MOZ-TIF2 leukemic cells. RT-PCR analysis for mouse *Brpf1* (left) and human *BRPF1* (right) of MOZ-TIF2 leukemic cells expressing WT human BRPF1, Δ 1–222 BRPF1 or empty vector, after transduction with mouse *Brpf1* shRNA. *Brpf1* shRNA significantly suppressed the expression level of mouse *Brpf1* but not human BRPF1. Data are mean \pm SD ($n = 3$). $^{***}P < .01$. **c** Efficiency of *Brpf1* knockdown by *Brpf1* shRNA on MOZ-TIF2 leukemic cells. Western blots for both mouse *Brpf1* and human BRPF1 in cell lysates from MOZ-TIF2 leukemic cells expressing WT human BRPF1, Δ 1–222 BRPF1 or empty vector, after transduction with mouse *Brpf1* shRNA. *Brpf1* shRNA significantly suppressed the expression level of mouse *Brpf1* but not human BRPF1. **d** Relative colony number of MOZ-TIF2 leukemic cells transduced with control shRNA or *Brpf1* shRNA. Knockdown of *Brpf1* resulted in reduction of colony formation. Overexpression of WT BRPF1 but not Δ 1–222 BRPF1 restored the colony formation activity of cells with downregulated *Brpf1*. Data are mean \pm SD ($n = 3$). $^{***}P < .01$. **e** Effects of *Brpf1* shRNA on expression of *Hoxa9*, *Hoxa10*, *Meis1* and *BRPF1* in MOZ-TIF2 leukemic cells expressing WT BRPF1, Δ 1–222 BRPF1 or empty vector. qRT-PCR showed that the expression level of *Hoxa9*, *Hoxa10* and *Meis1* was significantly suppressed by *Brpf1* shRNA, which was restored by overexpression of WT BRPF1 but not Δ 1–222 BRPF1. Data are mean \pm SD ($n = 3$). $^{***}P < .01$

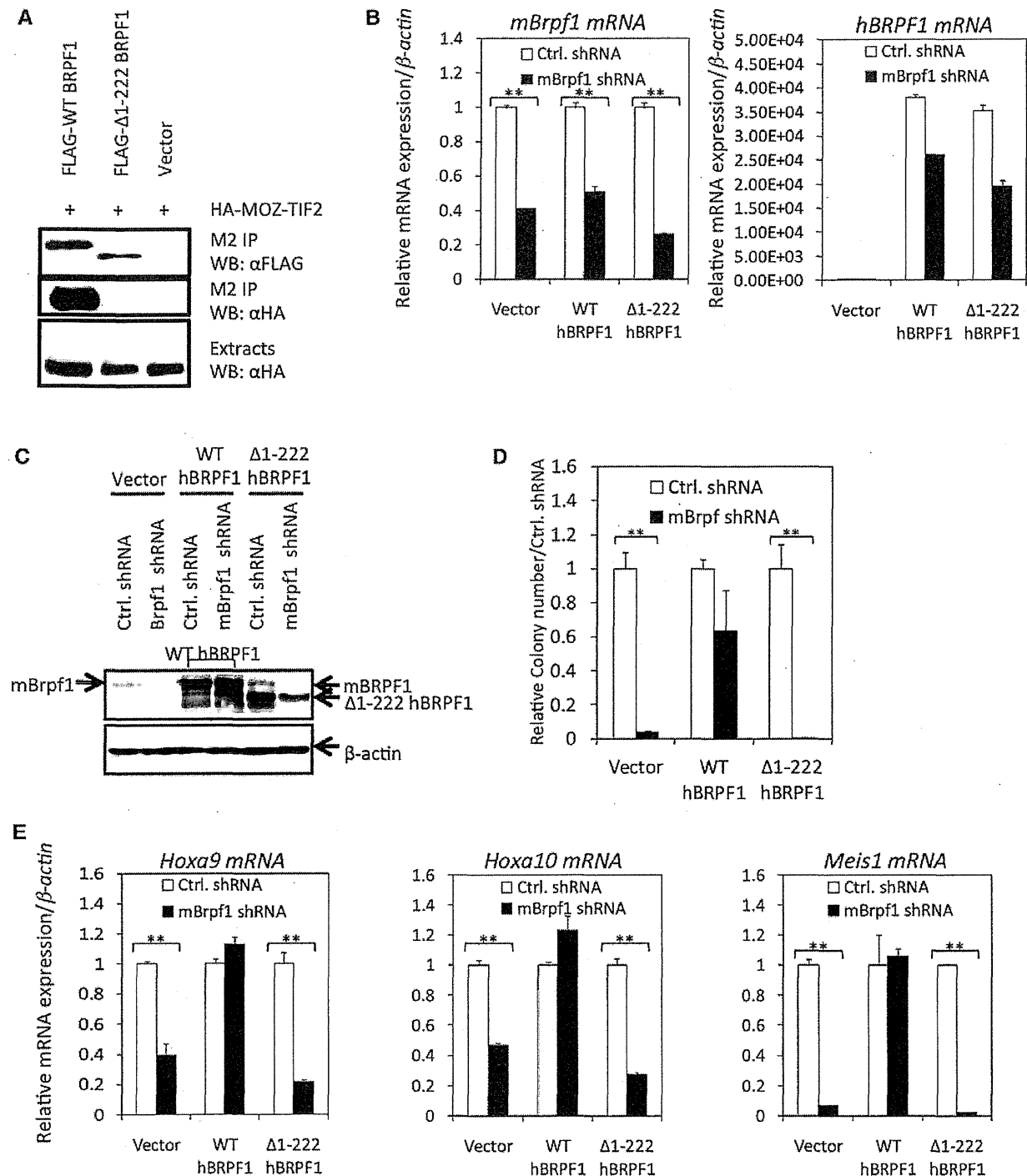
Bio)-coated plate. After 24 h of culture, cells were harvested and transplanted into sublethally irradiated recipient mice. The recipients were monitored for signs of leukemia (i.e., facial edema, lymphadenopathy, moribund, increase of GFP⁺ cells in peripheral blood).

Colony formation assay

The GFP⁺ infectants were sorted by cell sorter, and 1×10^4 of cells were cultured in 1 ml of methylcellulose media M3234 (Stem Cell Technologies) supplemented with 10 ng/ml of SCF, 10 ng/ml of IL-3, 10 ng/ml of GM-CSF (Peprotech). Number of colonies was monitored every 5–7 days of each replating using a DMIL inverted contrasting microscope (Leica). Cell sorting was performed using the cell sorter JSAN (Baybioscience). For the experiments using MSCV-neo vectors, infected cells were selected by adding G418 in the culture medium.

Brpf1 knockdown analysis

Brpf1 shRNA in lentiviral vectors was purchased from Openbiosystems. Viral particles were generated by cotransfection of 293FT cells with lentiviral packaging plasmids using Gene Juice (MERCK4Biosciences). $1\text{--}2 \times 10^5$ of MOZ-TIF2 leukemic cells were transduced with pLKO.1 vector or pLKO.1-*Brpf1* vector by



spinoculation at $2500\times g$ for 2 h at $32\text{ }^{\circ}\text{C}$ in virus containing medium supplemented with 8 ng/ml of polybrene. The cells were resuspended in StemPro-34 SFM medium (Invitrogen) containing cytokines (20 ng/ml SCF, 10 ng/ml OSM, 10 ng/ml IL-3) for 24 h. The infectants were plated in methylcellulose media supplemented with 10 ng/ml of

SCF, 10 ng/ml of IL-3, 10 ng/ml of GM-CSF, in the presence of puromycin ($4\text{ }\mu\text{g/ml}$) for selection of infected cells. Three days after selection with puromycin, 1×10^4 cells were plated in 1 ml of methylcellulose media and were proceeded to colony formation assay. The redundant infectants were used for qRT-PCR assay and

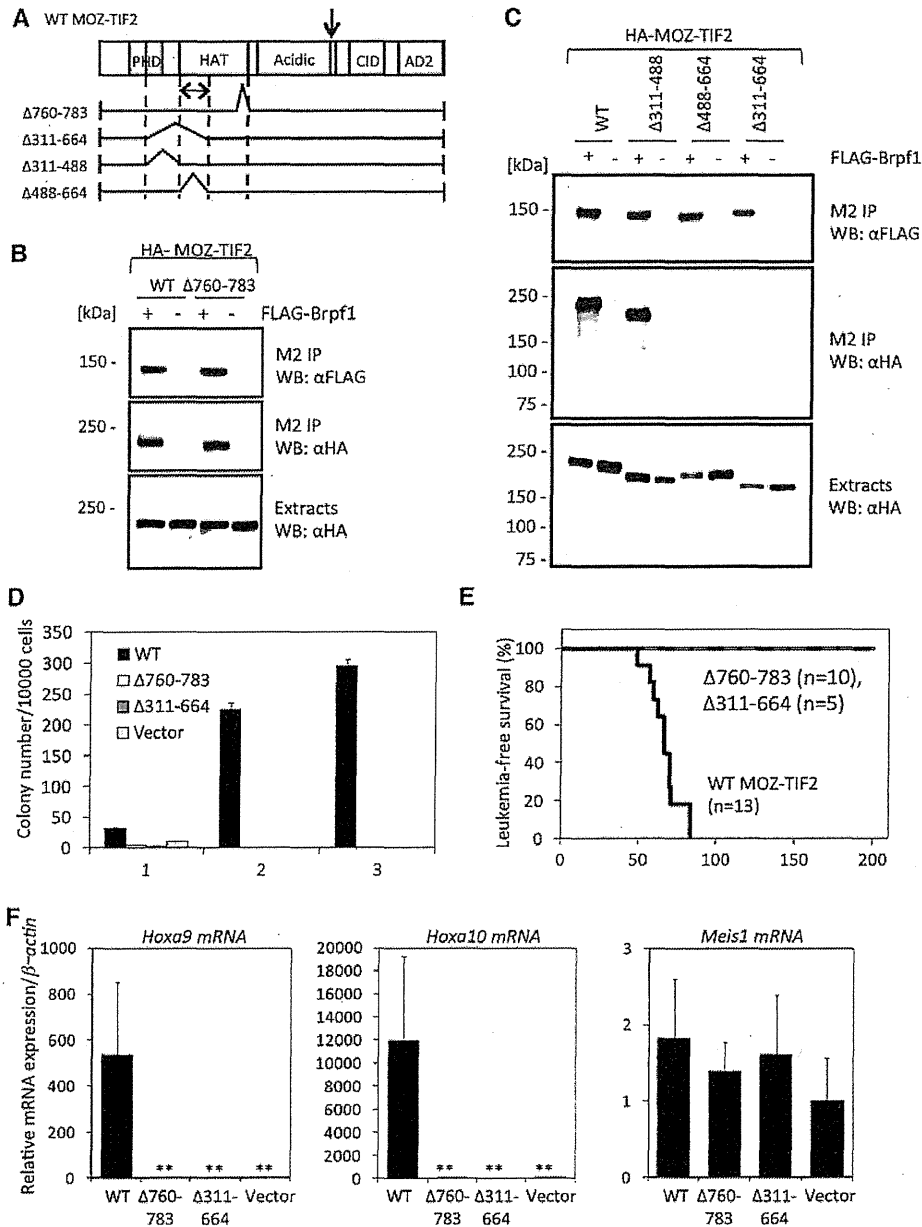


Fig. 2 Interacting domain of MOZ-TIF2 with Brpf1. **a** Structure of MOZ-TIF2 and its deletion mutants. **b** HA-tagged WT or $\Delta 760-783$ MOZ-TIF2 was cotransfected into 293FT cells together with FLAG-tagged Brpf1. Immunoprecipitates with anti-FLAG antibody (M2 IP) or cell lysates (Extracts) were subjected to immunoblotting with anti-HA or anti-FLAG antibodies. Both WT and $\Delta 760-783$ MOZ-TIF2 interacted with Brpf1. **c** HA-tagged WT or deletion mutants of MOZ-TIF2 were cotransfected into 293FT cells together with FLAG-tagged Brpf1. Immunoprecipitates with anti-FLAG antibody (M2 IP) or cell lysates (Extracts) were subjected to immunoblotting with anti-HA or anti-FLAG antibodies. MOZ-TIF2 containing N-terminal region of MOZ HAT domain (N488-664) interacted with Brpf1. **d** Number of colonies formed by cells transduced with WT, $\Delta 760-783$, $\Delta 311-664$

MOZ-TIF2 or empty vector. Both of the deletion mutants lost colony formation activity after 2nd round of replating. Data are mean \pm SD ($n = 3$). **e** Kaplan-Meier survival curve analysis of mice transplanted with WT, $\Delta 760-783$ or $\Delta 311-664$ MOZ-TIF2. All of the mice transplanted with WT MOZ-TIF2 developed AML, while all the mice transplanted with deletion mutants of MOZ-TIF2 survived without development of leukemia. **f** First round colonies of cells transduced with WT, $\Delta 760-783$, $\Delta 311-664$ MOZ-TIF2 or empty vector were collected and analyzed for expression levels of *Hoxa9*, *Hoxa10* and *Meis1* by qRT-PCR analysis. Increased expression levels of *Hoxa9* and *Hoxa10* were only observed in cells transduced with WT MOZ-TIF2. Data are mean \pm SD ($n = 3$). ****** $P < .01$

immunoblotting to determine the knockdown level of *Brpf1* or chromatin immunoprecipitation (ChIP) assay.

Quantitative real-time PCR (qRT-PCR) analysis

Total RNA was extracted using the RNeasy Mini Kit (Qiagen). The cDNA was reverse-transcribed using Superscript[®] VILO[™] (Invitrogen). Expression levels of genes were detected using the ABI 7500 Fast Real-Time PCR System with TaqMan[®] Gene Expression Assay Mixes (Applied Biosystems). β -actin was used as an internal control.

Immunoprecipitation and western blotting

For immunoprecipitation experiments, certain plasmids were co-transfected into 293FT cells by CaPO₄ co-precipitation. Cells were lysed in a lysis buffer [250 mM NaCl, 20 mM sodium phosphate (pH 7.0), 30 mM sodium pyrophosphate, 10 mM NaF, 0.1 % NP-40, 5 mM DTT, 1 mM PMSF, and protease inhibitor cocktail (Roche)], and cell lysates were incubated with anti-FLAG antibody-conjugated agarose beads (Sigma). After rotation at 4 °C overnight, and washing with lysis buffer, precipitated proteins were eluted by FLAG peptide and dissolved with SDS sample buffer. The blots were probed with anti-FLAG (M2) (Sigma), anti-HA (3F10) (Roche), anti-MOZ [], anti-Brpf1 (Sigma-Aldrich), or anti- β actin (clone AC-15) (Sigma) as primary antibodies, and horseradish peroxidase-conjugated secondary antibodies (SouthernBiotech). The bands were detected by chemiluminescence using ECL plus Detection Reagents (Amersham Biosciences).

Histone acetylation assay

Immunoprecipitates with anti-FLAG antibody obtained from 293FT cells transfected with FLAG-tagged WT or mutant MOZ were mixed with 50 mM Tris–HCl (pH 8.0), 10 % glycerol, 1 mM dithiothreitol, 0.5 μ l of [¹⁴C] acetyl-CoA (50 μ Ci/ml, Amersham), and 1 μ g of histone H2A, H2B, H3 and H4, respectively, and incubated at 30 °C for 1 h. After incubation, the samples were subjected to 15 % sodium dodecyl sulfate-PAGE, and the gels were analyzed for the levels of histone acetylation by BAS-2500 (FUJIFILM).

ChIP assay

Cells were fixed with 1 % formaldehyde for 10 min at room temperature and further incubated with 0.125 M glycine for 5 min to stop cross-linking reaction. Cells were then washed with ice-cold PBS containing protease inhibitor cocktail, centrifuged, and the pellets were lysed in lysis buffer (50 mM HEPES pH 7.5, 150 mM NaCl, 1 mM EDTA, 1 % Triton X-100, 0.1 % sodium deoxycholate, 0.1 % sodium

dodecyl sulfate, and protease inhibitor cocktail). The lysates were sonicated until the average DNA fragment length was 200–500 bp, using Branson Sonicator, diluted in 10 \times dilution buffer (1 % Triton X-100, 2 mM EDTA, 20 mM Tris–HCl pH 8.0, 150 mM NaCl and protease inhibitor cocktail), and incubated with antibodies at 4 °C overnight. On the following day, Dynabeads Protein G (Invitrogen) was added and incubated for another 6 h at 4 °C. The immunoprecipitates were washed twice with low salt buffer (0.1 % SDS, 1 % Triton X-100, 2 mM EDTA, 20 mM Tris–HCl pH 8.0 and 150 mM NaCl), once with high salt buffer (0.1 % SDS, 1 % Triton X-100, 2 mM EDTA, 20 mM Tris–HCl pH 8.0 and 500 mM NaCl) and finally twice with PBS containing 0.1 % Triton X-100. Bound chromatin was eluted in elution buffer (1 % SDS and 0.1 M NaHCO₃), and together with input DNA, crosslinking was reversed by overnight incubation at 65 °C with addition of 200 mM NaCl to the elution buffer. The eluted samples were then treated with 10 mM EDTA, 40 mM Tris–HCl (pH 6.5), and proteinase K (Roche) at 45 °C for 2 h. Finally, the immunoprecipitated and input DNA were extracted with phenol/chloroform extraction and ethanol precipitation, and analyzed by qRT-PCR using FastStart Universal SYBR Green Master (Roche) and 7500 Fast Real-Time PCR system.

Primer sequences are as follows.

Hoxa7 promoter:

Forward primer (F)/5'-GAGAGGTGGGCAAAGAGTG G-3', Reverse primer (R)/5'-CCGACAACCTCATACCTA TTCCTG-3'

Hoxa7 coding:

F/5'-CTGGACCTTGATGCTTCTAACT-3', R/5'-AGC CAGAGAAAGAGGGATTCTA-3'

Hoxa9 promoter:

F/5'-GAGCGGTTTCAGGTTTAATGC-3', R/5'-TGCCT GCTGCAGTGTATCAT-3'

Hoxa9 coding:

F/5'-GGTCCCCTGTGAGGTACATGT-3', R/5'-CAAA ACACCAGACGCTGGAA-3'

Hoxa10 promoter:

F/5'-CGGCCTTTGAGCCATAGGT-3', R/5'-GCCCCG CATTGATATAAATATGT-3'

Hoxa10 coding:

F/5'-TTCGGGCATCCCACTAAATG-3', R/5'-GGCCA CTCGGGCTGTATG-3'

Hoxa13 promoter:

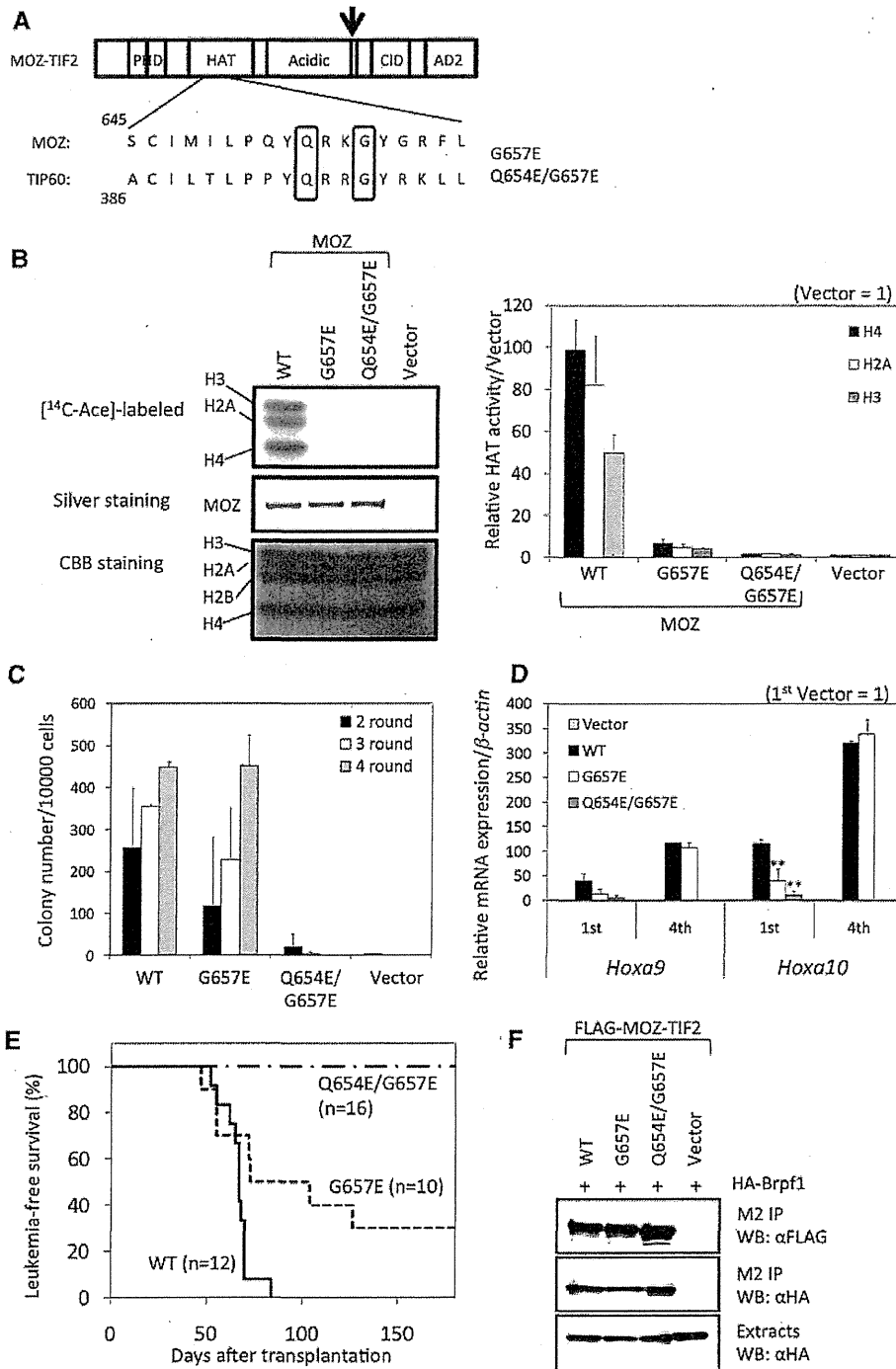
F/5'-TCCTTGGATGAGCGTTCTCT-3', R/5'-TGCAT GTTAAGTGCCTGCTC-3'

β -actin promoter:

F/5'-GCAGGCCTAGTAACCGAGACA-3', R/5'-AGTTT TGGCGATGGGTGCT-3'

Myf5 promoter:

F/5'-GGAGATCCGTGCGTTAAGAATCC-3', R/5'-CG GTAGCAAGACATTAAGTTCCGTA-3'



The antibodies used in these experiments are the same as written above for MOZ and Brpf1, and anti-acetyl-Histone H3 (Upstate), and anti-Histone H3 (abcam).

Statistical analysis

Statistical significance was determined by two-tailed Student *t* test.

Results

Brpf1 is required for immortalization of MOZ-TIF2 leukemic cells

Previous studies have suggested that BRPF1 forms complex with MOZ, and interacts directly to MOZ at N-terminal